REPORT DOCUMENTATION PAGE	Form Approved OMB NO. 0704-0188

Public reporting burden for this collection of information is estimated to average 1 hour per response, including the time for reviewing instructions, searching existing data sources, gathering and maintaining the data needed, and completing and reviewing the collection of information. Send comment regarding this burden estimates or any other aspect of this collection of information, including suggestions for reducing this burden, to Washington Headquarters Services, Directorate for information Operations and Reports, 1215 Jefferson Davis Highway, Suite 1204, Arlington, VA 22202-4302. and to the Office of Management and Budget, Paperwork Reduction Project (0704-0188), Washington, DC 20503.

1. AGENCY USE ONLY (Leave blank)	2. REPORT DATE	3. REPORT TYPE AND DATES COVERED
		FINAL PROGRESS REPORT 7/1/93 - 6/30/98

4. TITLE AND SUBTITLE	5. FUNDING NUMBERS
Spatial & Temporal Resolution in Near-Field Optical Microscopy	DAAH04-93-G-0194

6. AUTHOR(S)

Hans D. Hallen

7. PERFORMING ORGANIZATION NAMES(S) AND ADDRESS(ES)	8. PERFORMING ORGANIZATION REPORT NUMBER
North Carolina State University Department of Physics Raleigh, NC 27695-8202	

9. SPONSORING / MONITORING AGENCY NAME(S) AND ADDRESS(ES)	10. SPONSORING / MONITORING AGENCY REPORT NUMBER
U.S. Army Research Office P.O. Box 12211 Research Triangle Park, NC 27709-2211	ARO 31496.18-PH

11. SUPPLEMENTARY NOTES

The views, opinions and/or findings contained in this report are those of the author(s) and should not be construed as an official Department of the Army position, policy or decision, unless so designated by other documentation.

12a. DISTRIBUTION / AVAILABILITY STATEMENT	12 b. DISTRIBUTION CODE
Approved for public release; distribution unlimited.	

13. ABSTRACT (Maximum 200 words)

This project elucidated and examined the unique science behind the spectral and temporal contrast of near field scanning optical microscopy, illuminated the technology this enabled, and considered the limits of simultaneous position, time and spectral resolution. Specifically, (i) High-resolution, quantitative measurements of excess carrier lifetime in silicon were acquired in a novel, all-optical technique. The contrast in the images was modeled and is of interest since the resolution is significantly shorter than the carrier diffusion length. (ii) a Ti-sapphire laser has been constructed and modified to decrease pump power requirements so that measurements can be made before the carriers diffuse from under the probe. Novel electron-hole droplet effects are expected. (iii) Spectroscopic nano-Raman images were acquired for the first time. The Raman data illustrated interesting manifestations of a near-field in comparisons with far-field spectroscopy. (iv) The first and most thorough studies of the optical and thermal properties of near-field scanning optical microscope probes gave insights which led to the development of a new generation of high throughput probes. Other results reflect instrumentation advances: (v) A new constant linear motion system useful for NSOM or other probe microscope coarse approach. (vi) A new, low cost force feedback system. (vii) A nanometer-resolution, ~kHz bandwidth, millimeter range position sensor.

14. SUBJECT TERMS		15. NUMBER IF PAGES
Near Field Scanning Optical Microscopy, Instrument Design Pump-Probe Techniques, Temporal Resolution, Ramen Spectroscopy		10 pages
		16. PRICE CODE

17. SECURITY CLASSIFICATION OR REPORT	18. SECURITY CLASSIFICATION OF THIS PAGE	19. SECURITY CLASSIFICATION OF ABSTRACT	20. LIMITATION OF ABSTRACT
UNCLASSIFIED	UNCLASSIFIED	UNCLASSIFIED	UL

SPATIAL & TEMPORAL RESOLUTION IN NEAR-FIELD OPTICAL MICROSCOPY

FINAL PROGRESS REPORT

Hans D. Hallen

September 25, 1998

U.S. ARMY RESEARCH OFFICE

CONTRACT/GRANT NUMBER DAAH04-93-G-0194

NORTH CAROLINA STATE UNIVERSITY

APPROVED FOR PUBLIC RELEASE;
DISTRIBUTION UNLIMITED.

19981228 035

FORWARD

The near-field scanning optical microscope (NSOM) has many more capabilities than simply a subwavelength resolution optical microscope. The proximity of the metal-coated aperture probe to the sample changes the local electric field and thereby the interaction of light with the sample. This leads to differences between near field and far field measurements as have been observed in spectroscopy [1-3] and fluorescent lifetime [4] studies. These effects can be turned on and off by altering the distance between the probe and sample and so can provide a unique tool for the study of near-surface properties. Further, the resolution of the NSOM is such that one must carefully consider the length scales of the properties being measured, as the resolution may be shorter. This is the case in clean semiconductors for which the carrier diffusion length can exceed the measurement region. [5, 6] Finally, as with most members of the scanning probe family, a topographic image is simultaneously gathered. For NSOM, it acts as a complementary image to locate features of interest and to signal possible artifacts.

NSOM development was initially driven by the quest for better spatial resolution. Although the ultimate NSOM spatial resolution may not yet be a matter of consensus, a material limit for NSOM with metal apertures on the order of 12 nm for green light is generally accepted. [7] Efforts are still underway to increase this number, with claims below 1 nm using 'apertureless NSOM' techniques. [8, 9] These resolutions were only obtained at regions with sample topography, however. The best resolution of those techniques with molecularly flat samples (single fluorescent dye molecule) was still ~10 nm. [10] Perhaps more interesting developments from a scientific point of view are those mentioned above for which the physical measurement capabilities are increased through probe interactions, and those which aim to simultaneously provide resolution in several dimensions, including position, time and wavelength. It is useful at this point to consider what kinds of simultaneous temporal, spatial, and spectroscopic resolution can be achieved. The energy-time uncertainty principle limits the combined temporal and spectral resolution, and can be reached in some ultrafast studies. Spatial resolution does not present such a hard or straightforward barrier. Rather the signal intensity decreases rapidly as a function of the resolution divided by the wavelength. One must then take into account statistical and electronic noise to determine if a signal can be identified within some time duration, i.e., we must define an averaging time Δt_{ave}. This averaging time may be less than our temporal resolution, as in 1-shot acquisition, or it may be significantly longer if the process is made to repeat itself while averaging is performed. The maximum Δt_{ave} may be limited by either the desirable time sampling interval (e.g., in video-rate imaging) or by the instrument stability (e.g., in NSOM-Raman imaging), whichever is more restrictive. The choice of Δt_{ave} depends upon the probe in terms of the number of photons/second it delivers, the experimental cross section for the process under study, the collection efficiency, the time interval (time resolution), and the wavelength interval (spectral resolution). We do not quantify these here, but note that only two major variables can be optimized without affecting the data quality. These are: the maximum allowed Δt_{ave} and the amount of light output from the probe for a given aperture size (resolution).

This project was one of the major efforts focussing on NSOM developments which elucidated the difference between near-field and far-field measurements and pushed the limitations of simultaneous resolution in several variables. Raman spectroscopy requires fine spectral resolution, and exhibits spectral features absent in far-field or probe-retracted measurements. Carrier lifetime and carrier diffusion studies push the temporal envelope. Signal level is crucial to simultaneous reduction in several resolutions, and the insights gained from our probe studies have enabled new probe designs with much higher throughput.

STATEMENT OF THE PROBLEM STUDIED

At the start of this project, NSOM was a very immature technology. Imaging at far-subwavelength resolution had been demonstrated, but many possible contrast mechanisms such as the

temporal response of the sample and spectroscopy had not been investigated. There were no commercial instruments and the operation of most NSOM's was difficult and with low reliability. The object of this project was to investigate some new contrast mechanisms and to make necessary improvements to the NSOM instruments to improve reliability and stability. Some of the measurements performed required very long averaging times so would not have been possible without the extremely stable instrument developed. The choice of contrast mechanisms to focus upon was driven by the strengths of optical microscopy and technological needs.

Time resolution is important for technological reasons. One of the most common methods for assessing the quality of silicon is through the use of excess carrier lifetime. This can be done by injecting carriers with a pulse of light and detecting the excess carriers at a buried junction (optical beam induced carriers, OBIC), or by an all-optical technique which does not require buried devices. We chose the latter because it is more generally applicable for fresh wafers or even small areas within real device regions. The carrier diffusion process can also be imaged separately by using time-domain information to separate it from the lifetime effects.

One advantage of NSOM over many other proximal probe techniques is that it is possible to identify materials using spectroscopy. Whereas tunneling spectroscopy had been used in scanning tunneling microscopy (STM), it was not particularly sensitive to material properties. Atomic force microscopy (AFM) has little ability to differentiate species unless one undertakes a significant surface chemistry based approach, which works well only if the species on the surface are already known. Raman spectroscopy was chosen as it is one of the most powerful of the optical spectroscopies, providing species/phase identification by fingerprinting the spectra, stress information from peak shifts, and crystallinity from lineshapes. Further, it was not known if the near-field spectra would be the same as those in the far-field. IR spectroscopy complements Raman, so efforts were started in later years to develop aperture probes for the mid infrared (2 – 10 micron) regime.

The probe is the heart of an NSOM instrument, and it also is the limiting factor for resolution, light throughput, and signal intensity input. Studies of the thermal properties of the probe were required to identify the basis for source intensity limitations – where was all the energy being converted to heat? A higher input power with the same throughput would give more light (this turns out to be the most recent advance). We also have directed efforts to improving throughput efficiency.

As any developing technique, NSOM needed a wide variety of improvements. A compact coarse motion system for bringing the probe from millimeters away to submicron distances was required. The compact requirement stems from the stability requirement – that the drift during 10 hour images be ~ the aperture size. To test the motion of such a system to insure that the motion was fine (few nm step size) and smooth (so that the tip does not crash as it nears the surface), a position sensor was needed. The lateral force system in use at the start of the project was an optical lever arm detection of the motion of the diffraction pattern of the probe. The probe was oscillated at resonance. This system was tedious to align and very difficult if the probe was scanned rather than the sample. New methods for sensing the probe motion were required.

SUMMARY OF THE MOST IMPORTANT RESULTS

This project made considerable progress at advancing near field scanning optical microscopy through elucidation and study of the unique science behind the spectral and temporal contrast, by illuminating the technology which this enables, and considering the limits of simultaneous position, time and spectral resolution. Specifically,

(a) High-resolution, quantitative measurements of excess carrier lifetime in silicon have been acquired in a novel, all-optical technique. The contrast in the images has been modeled and is of interest since the resolution is significantly shorter than the carrier diffusion length.
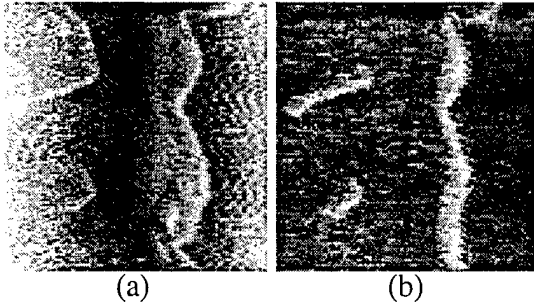
(a)   (b)

Figure 1: *Two images show the same 20 micron square region of an oxygen terminated silicon surface. (a) Topography with a 100 nm range (white higher). (b) Time-resolved image reveals regions near multiple step defects which have a faster recombination rate (0.038 nW range).*

(b) A Ti-sapphire laser has been constructed, modified to decrease pump power requirements, and successfully mode-locked with fsec-scale pulses for increasing the time resolution so that measurements can be made before the carriers diffuse from under the probe. Novel electron-hole droplet effects are expected.

(c) Spectroscopic nano-Raman images were acquired for the first time. The Raman data have illustrated the interesting manifestations of a near-field technique in comparisons with far-field spectroscopy.

(d) The first and most thorough studies of the optical and thermal properties of near-field scanning optical microscope (NSOM) probes gave insights which led to the development of a new generati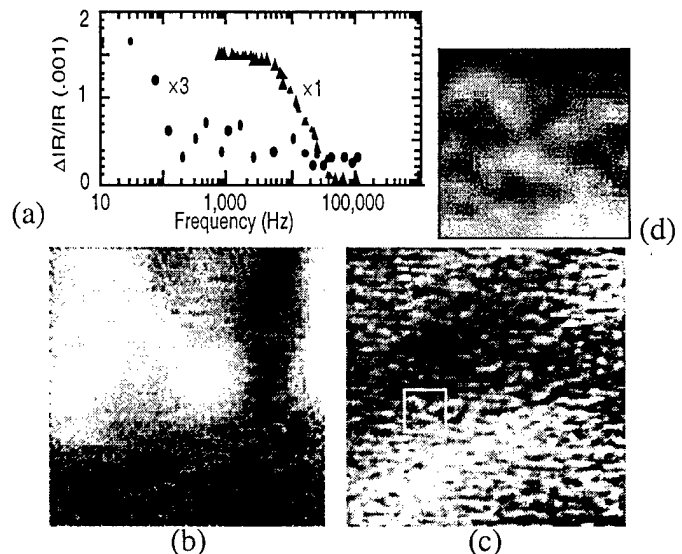on of high throughput probes. The thermal studies also indicate that the thermal processes are slow. This will positively impact the time-resolved capabilities of the NSOM technique.

(e) Other results reflect instrumentation advances required for next generation instruments including: (a) A new constant linear motion system useful for NSOM or other probe microscope coarse approach. (b) A nanometer-resolution, ~kHz bandwidth, millimeter range position sensor. (c) A new, low cost force feedback system for NSOM or AFM instruments.

We will consider each of these accomplishments in more detail.

(i) Excess Carrier Lifetime Measurements with NSOM.

Our efforts in time-resolved contrast have focused on studies of excess carriers in silicon which are created by an optical pulse. Time-resolved optical semiconductor characterization techniques with fine spatial resolution offer a unique opportunity to study the dynamics of carriers. We have developed such a technique by exploiting standard infrared carrier lifetime measurement methods in an NSOM. Sub-wavelength spatial resolution is provided by the NSOM, and the time-resolved sensitivity allows one to map carrier lifetime as a function of position. The technique can be used to locate any defects that reduce that lifetime locally. It results in a map of carrier dynamics that identifies the dominant processes as a function of position on the sample.

Carrier lifetime (τ) is defined as the average time excess carriers exist within a sample before they recombine and are thereby annihilated. During that time they contribute to the conductivity of a sample and may be collected in a device such as a photodetector.

Figure 2: *(a) The relative IR signal change vs. the visible light switching frequency for different samples. The samples with data as triangles and circles have effective lifetimes (from the knee) of 20 _sec and 1.6 msec, respectively. (b)-(c) The effects of varying the visible light switching frequency in 7.5 _m square images on the 'circle' sample. (b) The IR signal change image at 100 Hz is dominated by carrier recombination. (c) That at 20 kHz reflects carrier diffusion. (d) A detail from image (c), denoted by lines, one wavelength (of 1.15 _m IR) square.*
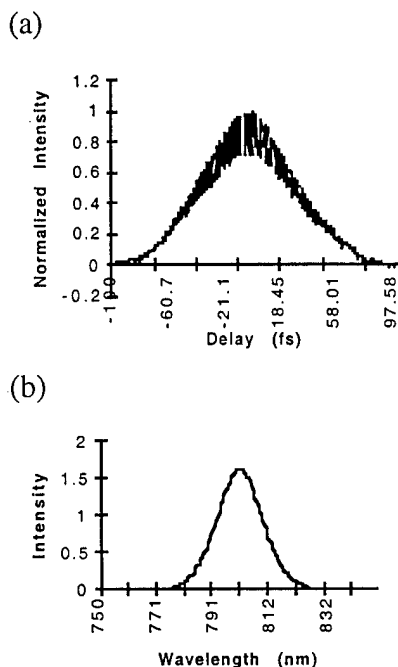
(a)

(b)

Wavelength (nm)

Figure 3: *(a) An autocorrelation trace from the Ti-sapphire laser. (b) The wavelength spread of the laser output.*

In our experiment [5, 6, 11-13], visible laser light is modulated to create a time-varying excess carrier distribution. This distribution is monitored by measuring its effect on continuous wave infrared (IR) laser radiation, also illuminating the sample. The photo-excited carriers scatter the IR light thereby reducing its intensity at the detector. Both visible and IR light are brought to the sample through the same NSOM probe aperture. This configuration insures high lateral resolution and avoids mismatch in the sample regions illuminated by either laser light. We record the change in the transmitted IR signal, $\Delta\phi_T$, as the visible light is switched on and off, using a lock-in amplifier. The magnitude of the change in the IR signal at a given visible light switching frequency is related to the lifetime. The samples used in these studies were oxidized silicon.

An example of this imaging technique is shown in figure 1. On the left is the topography and at the right the IR variation as the visible light is switched (related to carrier lifetime). Note that the carrier lifetime is reduced near some of the topographic steps seen in (a), as expected for steps in silicon. One can learn more by varying the frequency of the visible switching light. If the visible light is switched very rapidly, the carrier concentration does not have time to react and so the IR transmission will not change. At the opposite extreme, at very low visible light switching frequencies, the IR signal will change dramatically. The cross-over point w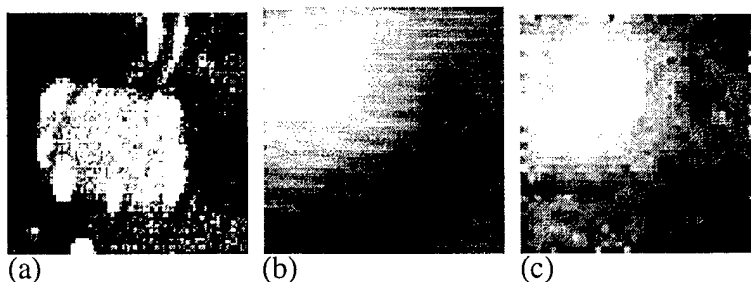ill be where the lifetime of the carriers is equal to the period of visible light switching. In figure 2(a) we show a plot of the IR signal variation as a function of frequency. More than one serial process is active in this region. One dominates on each side of the knee. It is interesting to compare an image taken with a visible switching frequency just below the knee compared to one taken at a frequency for which the slower process does not respond. This should allow imaging of the two processes independently, and is shown in the remainder of figure 2. Only the lifetime-related images are shown, as the topography was flat. The slower process, figure 2(b), clearly has a different spatial distribution than the faster process, figure 2(c). It is also interesting to note that the images at increasingly higher frequencies change only slightly, due to decreasing effects of the slower process. They are dominated by the same fast process evident in figure 2(a).

Using this technique it is possible to produce quantitative data in addition to qualitative high-resolution images. This is accomplished by noting the crossover (knee) frequency. We have compared the lifetime measured as the inverse of the knee frequency (a local measurement) to the average lifetime measurement for the entire sample using an independent method. We find agreement between our local method and the large-area technique for samples with lifetimes as different as 10 µs and 1.6 ms [13]. In summary, we have successfully

(a)   (b)   (c)

Figure 4. *Three images of a Rb doped KTP sample are shown. a) is a 10 micron square topographic image with a gray scale range of 17 nm, b) and c) are 4µm square images of the same corner of a Rb doped region. b) is a transmission image with a gray scale range of 460-550 nW and c) is a Raman image with a gray scale range of 18-22 cnts/sec obtained in the near-field.*
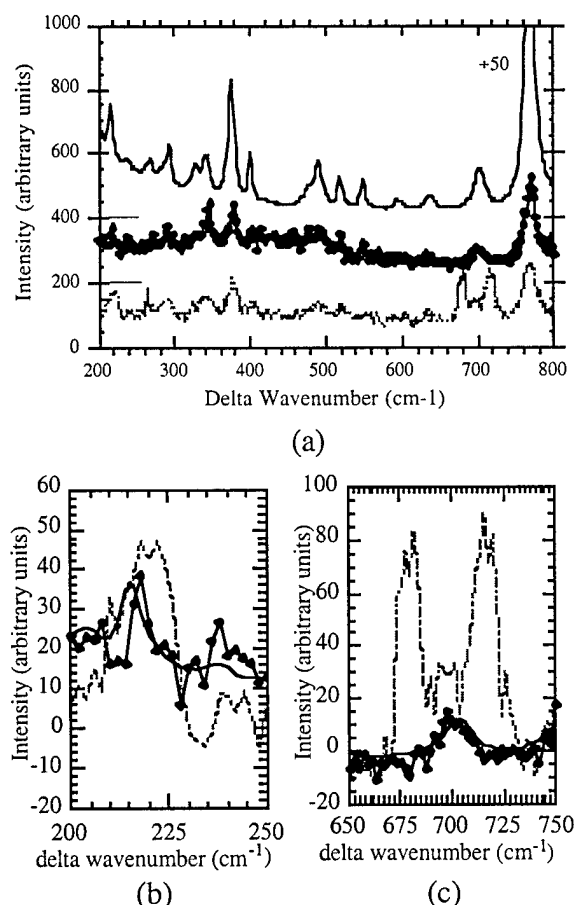
Figure 5. *A comparison of Raman spectra in the near-field vs. the far-field obtained in the KTP region. (a) The overview: the top (solid) curve is a microRaman spectrum while the lower two are obtained through a fiber probe with (middle, with points) the sample not in the near-field of the probe, and (bottom, dashed) the sample in the near-field of the probe. The baseline levels of each scan are indicated by horizontal lines on the left of the graph. (b,c) Portions of the spectra in (a) after scaling to overlay the large peak at 767 cm-1. The larger and shifted peak in the near-field data of (b) is due to an extra vibration mode which can be coupled to with longitudinally polarized light. The large split peaks in (c) cannot be explained by changes in coupling to modes, but is attributed to surface stresses and surface enhancement in the near-field.*

imaged the spatial distribution associated with carrier processes possessing different lifetimes, and quantitatively measured the lifetimes. This work drawn interest from several companies, including Phase Metrics, KLA Instruments, Micron Technology, and Westinghouse Electric Corporation.

(ii) Temporal resolution, the pulsed laser source.

The output of the lab-built Ti-sapphire laser has been coupled to a fiber after a grating pre-compressor to allow short pulses at the aperture of a near-field instrument. The design of the laser was modified from the 'standard' design to allow mode-locking at 2.5W. Of note in the arduous task of aligning the laser to self mode-lock is a recent paper which gives an estimate of the positions of the focusing cavity mirrors relative to the crystal. [14] Alignment and mode locking are easier and more stable with the new system. A paper describing the approach is in preparation. The base Ti-sapphire laser constructed for this project was based upon the 'standard' University of Washington design, [15, 16] with modifications by the ARO group of Henry Everitt at Duke. We have developed an alignment procedure, available on request. Pulse characterization includes monitoring the laser output with a fast photodiode, viewing a wavelength-smear with a CCD camera, and pulse autocorrelation in a Michelson geometry. We use a photodiode (or a blue LED) with a long wavelength cut-off in the blue to sense the autocorrelation. It is not sensitive to the laser wavelength, but does give a signal when two photons are simultaneously absorbed. Thus it serves as a simple electronic nonlinear detector to measure when the pulses from the two arms of the Michelson overlap. An autocorrelation trace is shown in figure 3. It shows that our pulse length is less than 50 fsec at the laser output. One can determine if the pulse is transform limited by the Heisenburg uncertainty relation by measuring the energy spread. Figure 3(b) shows a wavelength range of ~20 nm at ~800 nm which means the pulse would be transform limited at ~20 fsec.

(iii) Spectral Resolution, Raman and Infrared Spectroscopy.

Our efforts in Raman spectroscopic imaging [1-3, 11, 17] were made possible by our stable microscope. [18] We studied samples of KTP which were doped with Rb in several regions each 5 microns square. This results in a slight lattice expansion so that the topography could be corroborated with the optical data (the Rb doped region is ~12 nm higher). The index of refraction is also changed, allowing NSOM intensity images to also show the structures. Raman spectra obtained within and outside of the Rb doped regions, although similar, have distinct

Page 6

features. The height of the peak near 767 cm^{-1} is much higher for the Rb doped region. This fact can be used for imaging. The spectrometer was set to 767 cm^{-1}, and the NSOM probe scanned. The resulting Raman image (the first with an NSOM) is shown in figure 4. The acquisition time of this image was ~10 hours due to the required signal averaging. The stable design insured that the drift during this period was ~resolution of ~200nm. Several modifications are planned to make these measurements less time consuming and hence more generally applicable. We have proven that NSOM Raman spectroscopy and imaging are possible. Several important differences from standard far-field Raman spectroscopy were noted from this work. They include (i) concurrent and independent topographic imaging, (ii) surface enhancement, (iii) selection rule variation due to the presence of significant amounts of longitudinally polarized light, (iv) reduction in the Rayleigh tail due to the small sampled volume, and (v) spatial resolution. It was also found that the quality of the probe used in illumination mode could be deduced from the signal from the silica within the probe itself: the smaller the silica peak, the
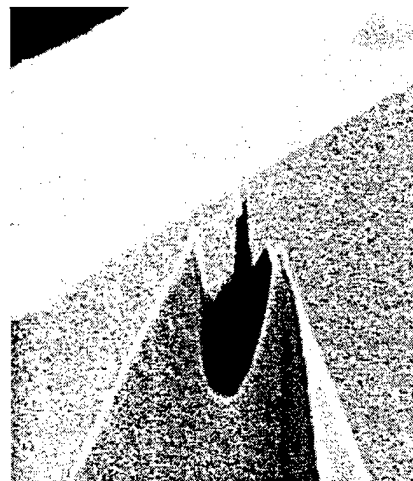

Figure 6: *A probe for mid-IR-NSOM machined from a silicon AFM probe which was coated with aluminum and subsequently milled with a focused ion beam. The annulus is ~0.5 micron in diameter. Note the sub-100 nm metal dot at the apex.*

better the probe. The explanation lies in a phase space argument for probe transmission. The differences can be illustrated in figures 4 and 5. Figure 5 shows a comparison between a conventional far-field microRaman spectrum, an NSOM Raman spectrum with the aperture brought away from the surface, and an NSOM Raman spectrum with the probe held in the near field. The spectrum through the NSOM aperture held in the far-field resembles the microRaman spectrum as it should. The near-field NSOM spectrum shows the properties noted above. The analysis is based upon the identification of mode symmetries and comparison of the near-field and far-field spectra.

The field of near field scanning optical microscopy (NSOM) in the visible spectral range is rapidly advancing, however progress has been much slower for wavelengths above ~1.5 μm due to probe problems, in particular the absorption of the silica in standard optical fibers. We have begun to develop NSOM probes usable through the mid IR spectral range. Several guiding principles drive our efforts: 1. fabrication and utilization of a metal dot or an annular aperture with metal in the center, 2. use of a large taper angle on a short probe, 3. use of a high index material, and 4. use of dielectric guiding where applicable. The key aspects of our IR probe tips will be: (i) a gross pyramidal shape, but more conical near the apex, (ii) made of a high

(a)
(b)
(c)
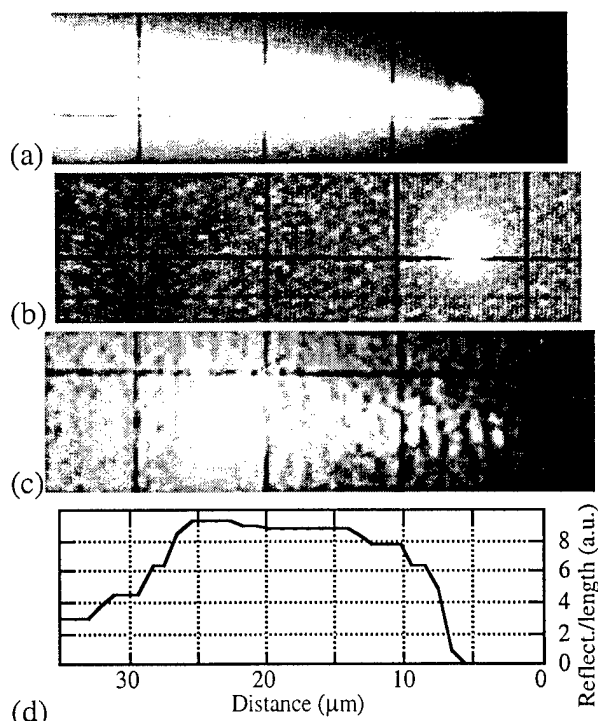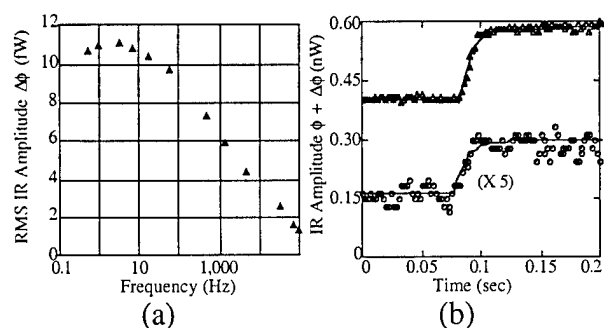(d)

Distance (μm)

Reflect./length (a.u.)

Figure 7: *Optical micrographs of a probe illustrate a typical (a) probe shape as viewed by external illumination, (b) optical emission of the same new aluminum coated probe from a point at the end, and (c) the optical emission of the same probe after damage by coupling 14 mW of green light into the probe. The scale of the dark grids in the micrographs is 10 μm per box. For comparison, the results of a ray tracing model which counts the number of ray bounces per length is shown in (d).*

Figure 8. *The change in IR signal* $\Delta\phi$ *is measured as a function of (a) frequency (before damage) and (b) time. The fits shown in (b) yielded time constants of 10.3 and 10.1 msec for the triangles (after damage) and circles (before damage) respectively.*

index material, (iii) supported by a cantilever much like many AFM probes, (iv) high throughput, and (v) capable of handling relatively large input powers. To confine the optical field, the pyramids and cantilever will be coated with a metal on one side. A small aperture or annulus is subsequently ion milled into the metal coating at the apex of the tip. A small metal dot is left at the apex, which will both improve resolution and throughput. The Focused Ion Beam (FIB) facility at NCSU is used to fabricate tips with the central and the open part of the annulus having dimensions as small as 50 nm. This approach to tip manufacturing for the IR spectral range is distinctly different from the usual practice of pulling fibers or capillaries as utilized in the visible spectral range, or as practiced by competing IR efforts. It is indeed a radical departure from previous approaches but will meet all the goals outlined above in the repeatable production of well-characterized probes. One of our first probes is shown in figure 6.

(iv) Thermal Properties of the Probe.

The configuration for measuring the temporal dependence of a sample process is very similar to that which can be used to investigate the temporal behavior of the probe. [19-21] The silicon wafer is moved to the other side of the collection lens, where it serves as an infrared transmission filter. The probe is cyclicly heated by the pulsed visible light (through absorption in the Al-coated taper). This same heating is the origin of thermally induced failure of probes, which can be investigated by this method. Thermal expansion of the probe and change in the optical properties of the Al coating result from the heating. For modeling purposes, these can be divided into an elongation of the probe (reduces IR throughput), increasing the probe radius (increases IR throughput), and Al reflectivity reduction (decreases IR throughput). The former two occur together, but the effects on the IR throughput differ. We have seen examples of increases and decreases of the IR signal as the visible light is turned on. Often the correlation changes sign as the probe is slowly destroyed by thermal diffusion of the Al into islands, indicating (as modeling suggests) that the effects have nearly equal importance. Using a model calculation, the tip temperature can be estimated, and the results agree with other recent studies. Ray tracing studies indicate that the location of maximal power input to the probe occurs tens of microns from the tip, suggesting that modifications to the geometry may help. Experiments concur, figure 7. Another important feature is the time-scale of the heating. Measurements of the time dependence of the IR response, figure 8, indicate that the system is can be modeled only approximately by a single time constant, but the 10-20 msec time scale is very long.

This long thermal time scale of the probe has implications for the time-resolved work. It indicates that the sample and probe effects may be separated in the time domain. It also has implications for using pulsed lasers in NSOM. If the pulse repetition rate is fast compared to thermal diffusion rates, the probe response will average the power, allowing short, high energy pulses to be used.

(v) Novel aspects of the NSOM.

(a) **Constant linear motion system.** One of the problems with inertial sliders and stepper motor coarse approach mechanisms (as almost universally used in scanning probe microscopes) is that to guarantee that the probe is not crashed during approach, one must step the coarse system then search with the fine approach system to insure that a crash will not occur during another coarse step. The step-search-step-... method is slow. Often the search is not done and the probe will suffer a slight or occasionally a major crash during approach, reducing reliability and possibly creating artifacts in the data. A continuous motion of the probe would be fast and alleviate the need for a search. We developed such a motion system during this year (paper in preparation). It is most simply described as walking with dragging feet. Eight feet hold the scanner system (Figure 9a). Each is driven by a shear piezo with a saw-tooth wave. The waves are out of phase so that most of the time all eight feet move continuously forward with individual feet snapping back when they reach their full extension (Figure 9b). The friction on the other seven feet overcome that of the eighth, aided by inertia, so that the scanner

Figure 9. *(a) the drive voltages for the eight feet are out-of-phase saw tooth waves. (b) The scanner assembly can move a distance limited only by the length of the polished tube. It is supported solely by the eight shear-piezo- and sapphire hemisphere-feet.*

system continues forward (with few nm jiggles). The range of the scanner is limited by the length of the polished steel (or sapphire plate) supporting the scanner system. Several important details are required to make the system work: (1) The feet must slide as they individually retract (or extend if moving the other direction). This requires proper surface preparation and enough motion that the elasticity in the foot and its mount is not overcome by the contact static friction. The latter requires that the force not be too high and that the driving voltage on the piezo is large enough (we use 400-1000 V). The wave-form must be sharp so that the inertial effects help. The forces on all the feet must be the same to prevent the scanner assembly from following one foot back and forth. (2) The mounting structure should not provide force along the direction of travel. If the 4 feet spring-held against the top are not mounted correctly, the structure will twist and an axial force will build up, impeding the motion. This problem results in a motion in both direction which slows and stops after a short distance. If the mounting structure pushes in one direction, motion favoring or only in that direction will result. (3) The scanner structure must be held tightly enough that the motion is controlled. Inertial effects from the fine motion system can slide the scanner if it is loose. We have also found a hysteresis of the motion if it is too loose: after traveling in one direction, the motion will continue in that direction for a period before reversing as the feet are nominally moving the scanner system in the opposite direction. A properly adjusted system is robust over a large range of piezo driving voltages and saw-tooth wave frequencies. A typical motion is shown in Figure 10. We have observed its motion while immersed in liquid nitrogen (after adjusting for room temperature motion), which demonstrates the unusual robustness of the design.
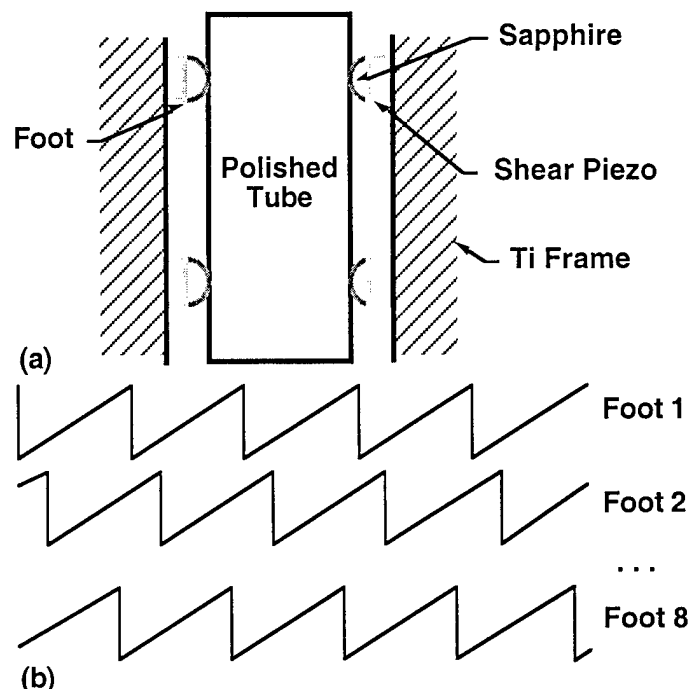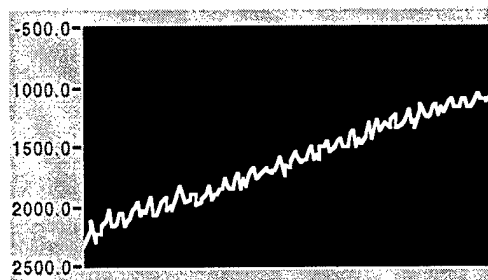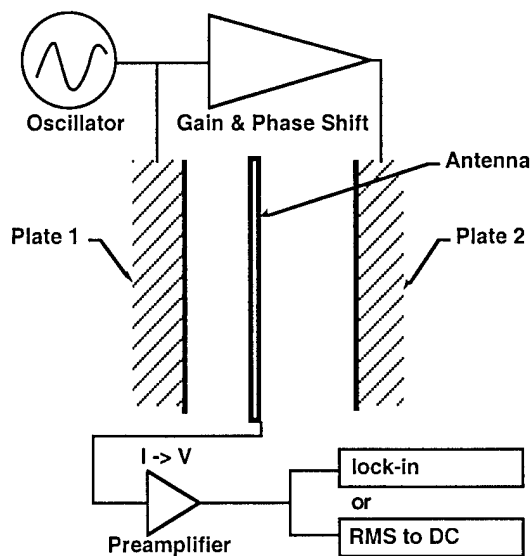

Figure 10. *The motion of the scanner system over a few-second interval. The vertical axis is approximately twice the displacement in nm. The motion is linear except for small (~10-60 nm) excursions as the feet individually retract.*

Figure 11. *Schematic of a position sensor.*

(b) **Position sensor.** A compact position sensor has been developed with performance that exceeds most commercial products and is compatible with scanning probe microscopes. Features of note include sub-nanometer noise in a fairly wide (~kHz) bandwidth, linearity with position, operation over relatively long distances (few millimeter -- more with less sensitivity *or* bandwidth), non-contact operation (except for one wire), and a very compact size. A schematic is shown in Figure 11. An antenna is mounted on the moving part between two plates held fixed. An oscillator drives one plate while a gain and phase-shifted (near 180°) version drives the other. The current coming from the antenna is measured with high gain (lock-in amplifier or RMS-to-DC converter), and zeroed by adjusting the drive signal to the second plate. The signal will linearly depart from zero as the moving part linearly moves. The calibration and hence sensitivity (noise is constant and dominated by the current preamplifier (in our system) and/or noise pick-up) increase as the plates are brought closer together, as the antenna area increases, as the plate drive voltage increases, and as the plate drive voltage frequency increases -- since the coupling to the antenna is by capacitance. The gain of the current preamplifier (and later stages) also is important. The current preamplifier or conversion to DC (by RMS chip or lock-in) determines the bandwidth. The latter dominates in our system.

(c) **Force feedback system.** One of the reliability problem areas for NSOM instruments has been the probe to sample distance regulation system. We have addressed this problem in this project by modifying a novel design by Julia Hsu's group at the University of Virginia. [22] We improved the signal to noise ratio, and eliminated the need to dedicate an expensive lock-in amplifier for the distance regulation subsystem. [23] The technique involves the measurement of the impedance of a piezoelectric element driving the probe at resonance. As the probe interacts with the sample, a force is generated at the resonant frequency. This effects the impedance of the piezo, which is detected in a bridge configuration. The current induced by the driving voltage is compared to a phase-shifted copy of the drive voltage, and the difference amplified, filtered, and converted from the resonant frequency ~50 kHz to low frequencies in a commercial RMS converter chip. This output is tuned to zero with a retracted probe, and its offset from zero used to drive a feedback circuit. This scheme seems to greatly improve reliability and provide consistent low noise topographic images. The new method for measuring the impedance changes offers several improvements over previous designs: (1) a lock-in amplifier is not required -- it is replaced with an inexpensive RMS to DC chip, (2) improved stability of the instrument versus time and temperature, (3) reduced noise, and (4) a more compact electronics package. Figure 12 shows data from this new method. Note that the noise levels in the topographic image are in the sub-nanometer range.
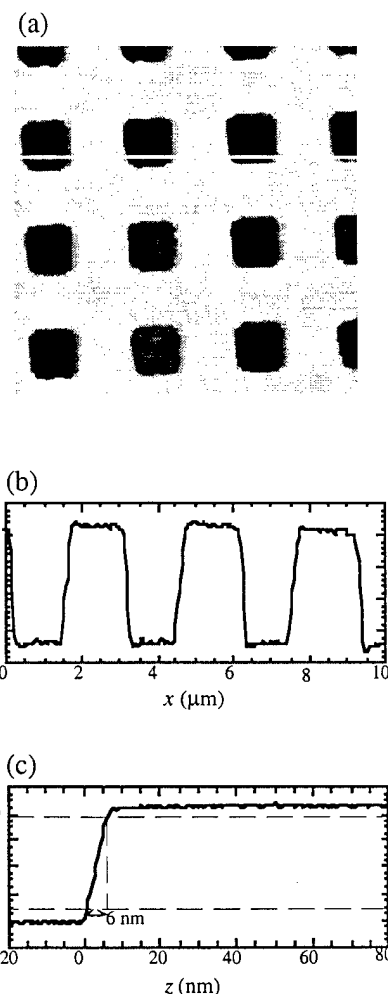
(a)

(b)

(c)

Figure 12: *a) An image of a 2D grating taken with an NSOM tip using the new feedback. The grayscale represents 25 nm height difference. (b) A line cut of height changes versus distance (x), as indicated in Fig. 2(a). (c) Error signal as a function of tip-sample separation (z). The zero of z is defined by the position at which the bridge output signal saturates, i.e., tip-sample "contact" point. The 10% and 90% of the transition are marked on the graph. The corresponding tip-sample separation is ~ 6 nm.*

LIST OF MANUSCRIPTS SUBMITTED OR PUBLISHED UNDER ARO SPONSORSHIP DURING THIS PROJECT, INCLUDING JOURNAL REFERENCES:

Refereed Journals

1. J. W. P. Hsu, A. A. McDaniel, H. D. Hallen, "A Shear Force Feedback Control System for Near-field Scanning Optical Microscopes without Lock-in Detection," Review of Scientific Instruments **68** (8), 3093-3095 (1997).
2. A.H. La Rosa, B. I. Yakobson, H.D. Hallen, "Optical imaging of carrier dynamics with sub-wavelength resolution," Appl. Phys. Lett. **70** (13), 1656-1658 (1997).
3. C.L. Jahncke and H.D. Hallen, "A versatile, stable scanning proximal probe microscope," Review of Scientific Instruments, **68** (4), 1759 (1997).
4. C.L. Jahncke, H.D. Hallen, and M. A. Paesler, "Nano-Raman spectroscopy and imaging with the near-field scanning optical microscope," An invited contribution to the J. Raman Spectroscopy, **27**, 579-586 (1996).
5. B.I. Yakobson, A. La Rosa, H.D. Hallen, and M. A. Paesler, "Thermal/optical effects in NSOM probes," Ultramicroscopy **59**, 334 (1995).
6. A. La Rosa, B. I. Yakobson, and H.D. Hallen, "Origins and effects of thermal processes in near-field optical probes," Appl. Phys. Lett. **67**, (18), 2597-2599 (1995).
7. C.L. Jahncke, M. A. Paesler, and H.D. Hallen, "Raman imaging with near-field scanning optical microscopy," Appl. Phys. Lett. **67**, (17), 2483-2485 (1995).
8. H. D. Hallen, A. La Rosa, and C.L. Jahncke, "Near-field scanning optical microscopy and spectroscopy for semiconductor characterization," Physica Status Solidi (a) **152**, 257-268 (1995).
9. A. La Rosa, C.L. Jahncke, and H.D. Hallen, "Time as a contrast mechanism in near-field imaging," Ultramicroscopy **57**, 303-308 (1995).

Conference Proceedings

1. M.A. Paesler, H.D. Hallen, B.I. Yakobson, C.J. Jahncke, P.O. Boykin, and A. Meixner, "Near-field optical spectroscopy: enhancing the light budget," Microscopy and Microanalysis **3**, 815 (1997).
2. C.L. Jahncke and H. D. Hallen."Near-field Raman Spectra: surface enhancement, z-polarization, fiber Raman background, and Rayleigh scattering", 9th annual meeting of IEEE Lasers and Electro-Optics Society (LEOS) 96 conference proceedings volume 1, pp. 176-177.
3. A. La Rosa, B. I. Yakobson, H.D. Hallen, "Imaging of carrier dynamics with near-field scanning optical microscopy," Mat. Res. Soc. Symp. Proc. **406**, 189-194 (1996).
4. H.D. Hallen, B. I. Yakobson, A. LaRosa, and M. A. Paesler, "Thermal/temporal response of the NSOM probe/sample system," SPIE Proceedings **2535**, 34-37 (1995).
5. A. La Rosa, C.L. Jahncke, and H.D. Hallen, "Time-resolved contrast in near-field scanning optical microscopy of semiconductors," SPIE Proceedings **2384**, 101-108 (1995).

Book Chapters, etc.

1. H.D. Hallen and M. A. Paesler, "Lens," an article for *The Macmillan Encyclopedia of Physics*, edited by John S. Rigden (Macmillan, New York, 1996).

Theses

1. "Near-field Optical Spectroscopy," Catherine Jahncke

2. "Time-resolved Near-field Imaging of Carrier Dynamics in Silicon" Andres LaRosa

LIST OF ALL PARTICIPATING SCIENTIFIC PERSONNEL SHOWING ANY ADVANCED DEGREES EARNED BY THEM WHILE EMPLOYED BY THIS PROJECT

Faculty Participants: Hans D. Hallen, Boris I. Yakobson

Graduate Student Participants:
    Andres La Rosa, graduated with Ph.D, June, 1996
    Catherine Jahncke, graduated with Ph.D, June, 1996
    Michael Muto, graduated with M.S, June, 1997
    Sean Boylan, M.S. candidate
    Eric Ayars, Ph.D. candidate

REPORT OF INVENTIONS (BY TITLE ONLY)

1. "Signal detection for an alignment-free atomic force microscope" was invented and a patent disclosure statement prepared.
2. "A high throughput, high input power and high resolution IR probe for IR Near Field Scanning Optical Microscopy (IR-NSOM)" was invented and a patent disclosure statement prepared.
3. "A variable temperature electrically driven constant velocity translator with nanometer-scale precision" was invented during this project and we are considering a patent disclosure statement.

BIBLIOGRAPHY

[1] C.L. Jahncke, M.A. Paesler and H.D. Hallen, Appl. Phys. Lett. **67**, 2483 (1995).
[2] C.L. Jahncke and H.D. Hallen, Bull. Am. Phys. Soc. **40**, 685 (1995).
[3] C. L. Jahncke, H. D. Hallen and M. A. Paesler, J. of Raman Spectroscopy **27**, 579 (1996).
[4] X. Sunney Xie and Robert C. Dunn, Science **265**, 361 (1994).
[5] A. H. LaRosa, B. I. Yakobson and H. D. Hallen, Mater. Res. Soc. Symp. Proc. **406**, 189 (1995).
[6] A.H. LaRosa, B.I. Yakobson and H.D. Hallen, Appl. Phys. Lett. **70**, 1656 (1997).
[7] E. Betzig, J.K. Trautman, T.D. Harris, J.S. Weiner and R.L. Kostelak, Science **251**, 1468 (1991).
[8] F. Zenhausern, M.P. O'Boyle and H.K. Wickramasinghe, Appl. Phys. Lett. **65**, 1623 (1994).
[9] F. Zenhausern, Y. Martin and H.K. Wickramasinghe, Science **269**, 1083 (1995).
[10] H.K. Wickramasinghe, personal communication.
[11] H. D. Hallen, A. H. La Rosa and C. L. Jahncke, Phys. Stat. Sol. (a) **152**, 257 (1995).
[12] A. LaRosa, C.L. Jahncke and H.D. Hallen, Ultramicroscopy **57**, 303 (1995).
[13] A.H. LaRosa, C.L. Jahncke and H.D. Hallen, SPIE Proceedings **2384**, 101 (1995).
[14] Ivan P. Christov, Vency D. Stoev, Margaret M. Murmane and Henry C. Kapteyn, Optics Lett. **20**, 2111 (1995).
[15] Melanie T. Asaki, Chung-Po Huang, Dennis Garvey, Jianping Zhou, Henry C. Kapteyn and Margaret M. Murmane, Optics Letters **18**, 977 (1993).
[16] Kendall Read, Florian Blonigen, Nicole Riccelli, Margaret Murmane and Henry Kapteyn, Optics Letters **21**, 489 (1996).
[17] C.L. Jahncke and H.D. Hallen, Proceedings of 9th annual meeting of IEEE Lasers and Electro-Optics Society (LEOS) 96, **1**, 176 (1996).
[18] C.L. Jahncke and H.D. Hallen, Rev. Scient. Instr. **68**, 1759 (1997).
[19] A. H. LaRosa, B. I. Yakobson and H. D. Hallen, Appl. Phys. Lett. **67**, (1995).
[20] H.D. Hallen, B.I. Yakobson, A. LaRosa and M.A. Paesler, SPIE **2535**, 34 (1995).
[21] B.I. Yakobson, A. LaRosa, H.D. Hallen and M.A. Paesler, Ultramicroscopy **61**, 179 (1995).
[22] J.W.P. Hsu, M. Lee and B.S. Deaver, Review of Scientific Instruments **66**, 3177 (1995).
[23] J. W. P. Hsu, A. A. McDaniel and H. D. Hallen, Rev. Sci. Instr. **68**, 3093 (1997).